BMC Nephrology

RESEARCH

Open Access

Construction and validation of a predictive model for malignant tumors in patients with membranous nephropathy

Yaling Zhai[1,2†], Shuaigang Sun[1,2†], Wenhui Zhang[1,2], Huijuan Tian[1,2] and Zhanzheng Zhao[1,2*]

Abstract

Background The association between membranous nephropathy (MN) and malignant tumors has long been focused. However, most existing studies have primarily concentrated on patients diagnosed with malignant tumors within a limited timeframe, typically defined as one year before or after the diagnosis of MN. This narrow focus only captures a subset of MN patients complicated by malignant tumors, leaving those diagnosed outside this timeframe understudied and largely unexplored. In the present study, we aim to comprehensively investigate the clinicopathological characteristics of MN patients complicated with malignant tumors and to develop an effective predictive model for identifying the risk of malignancy in MN patients.

Methods A retrospective analysis was conducted on the demographic, clinical, and pathological characteristics of 174 MN patients complicated with malignant tumors and 604 idiopathic membranous nephropathy (IMN) patients without malignant tumors. All patients were randomly allocated into a training cohort ($n=584$) and a validation cohort ($n=194$) in a 3:1 ratio. A predictive model was developed using regression analysis, and its performance was evaluated in terms of discrimination, calibration, and clinical utility through the area under the ROC curve (AUC), calibration curve, and decision curve analysis (DCA).

Results MN patients complicated with malignant tumors demonstrated significantly increased deposition rates of glomerular IgG1, IgG2, IgG3, and PLA2R, as well as decreased deposition rates of IgG4. Based on independent risk factors, a predictive model was developed, which exhibited excellent performance upon validation.

Conclusion In this largest cohort to date of MN patients with malignant tumors, a predictive model was constructed using pathological parameters to estimate the risk of malignancy effectively. This tool aims to assist clinicians in decision-making and improve the prognosis of high-risk MN patients by facilitating tumor screening at the time of initial diagnosis.

Keywords IgG subclasses, Malignant tumor, Membranous nephropathy, PLA2R, Predictive model

†Yaling Zhai and Shuaigang Sun contributed equally to this work.

*Correspondence:
Zhanzheng Zhao
zhanzhengzhao@zzu.edu.cn
[1]Department of Nephrology, The First Affiliated Hospital of Zhengzhou University, Zhengzhou, China
[2]The Renal Research Institution of Zhengzhou University, Zhengzhou, China

Introduction

Membranous nephropathy (MN), pathologically characterized by diffuse thickening of the glomerular basement membrane and subepithelial IgG deposition, is the most common cause of nephrotic syndrome (NS) in adults, accounting for 38.18% of cases, particularly among middle-aged and elderly populations [1]. Over the past decades, the incidence of MN has exhibited a marked rising trend across all age groups, with the most notable increase observed in younger individuals [2].

In 1966, Lee first elucidated the relationship between NS and malignant tumors in a large-scale study. Of the 101 nephrotic syndrome patients included, 11 were found to have concomitant malignant tumors, and remarkably, MN was identified as the predominant pathological type in 82% of these cases [3]. This observed rate of malignancy was significantly higher than the expected incidence for this age cohort. Furthermore, a recent study by Lefaucheur et al. reported that the risk of malignant tumors in MN patients was approximately ten times higher than in the general population, irrespective of age or sex [4]. Over the years, numerous studies have consistently highlighted the association between MN and malignant tumors, with most malignancies identified either simultaneously with MN diagnosis, shortly thereafter, or even prior to MN onset. Interestingly, it has also been reported that certain patients were diagnosed with malignant tumors within 12 months after MN manifestation [5–6], suggesting a more complex relationship. However, we found that malignant tumors can occur at any time in MN patients, underscoring the need for further investigation into this association. Such research is vital for the timely detection of malignant tumors in high-risk MN patients, enabling clinicians to avoid unnecessary immunosuppressive therapies [7].

Attempting to find novel non-invasive biomarkers and early detection methods for potential malignant tumors in MN assumes paramount significance in terms of patient treatment and prognosis. M-type phospholipase A2 receptor (PLA2R) and thrombospondin type-1 domain-containing 7 A (THSD7A), confirmed as two primary pathogenic podocyte target antigens in idiopathic membranous nephropathy (IMN) [8–9], however, recent studies have also indicated the occurrence of malignant tumors in PLA2R and THSD7A-associated MN [10], which challenge the designation of PLA2R and THSD7A as markers of primary MN and further underscore the intricate nature of the association between malignant tumors and MN.

Previous studies have proposed that the absence of glomerular PLA2R deposition, negative circulating anti-PLA2R antibodies, strong glomerular IgG1 and IgG2 deposition, and the lack of IgG4 deposition may serve as independent predictors of malignancy in MN patients [11, 12, 13, 14, 15]. However, the conclusions of these studies have been inconsistent, likely due to limited sample sizes and variations in study design.

In this study, we conducted a comprehensive analysis of the demographic, clinical, and pathological characteristics of MN patients with and without malignant tumors, utilizing the largest sample size to date. Specifically, we evaluated circulating anti-PLA2R antibodies, glomerular PLA2R deposition, and glomerular IgG subtype deposition. Furthermore, we aimed to develop a novel and reliable predictive model to assist clinicians in decision-making, facilitating early tumor screening at the time of initial MN diagnosis and improving outcomes for high-risk patients.

Materials and methods

Study subjects

This retrospective study utilized electronic medical records to identify patients diagnosed with MN and malignant tumors who were admitted to the First Affiliated Hospital of Zhengzhou University between January 1, 2014, and September 1, 2023. Patients in the malignant tumor group were included based on the following criteria: (i) Initial onset of MN. (ii) Diagnosis of MN confirmed by renal biopsy. (iii) A previous history of malignant tumors, or newly diagnosed malignant tumors identified during at least 1 year of follow-up. The exclusion criteria were: (i) Presence of other glomerular diseases (e.g., IgA nephropathy or mesangial proliferative glomerulonephritis). (ii) Secondary MN (e.g., MN associated with systemic lupus erythematosus, chronic hepatitis B or C, or exposure to drugs or toxicants). (iii) Absence of essential pathological diagnostic parameters. Cases where certain indicators were missing but the rest of the renal pathology report was complete, were not excluded. For the control group, we included patients diagnosed with IMN confirmed by renal biopsy between January 1, 2015, and June 1, 2018, in our hospital. These patients had no history of malignant tumors and remained free of malignancies during a minimum follow-up period of 1 year. Figure 1 shows the detailed flowchart of this study.

Clinical data collection

Baseline demographic, clinical, and pathological data were collected at the time of the first diagnosis of MN via renal biopsy. Demographic data included age and sex. Clinical data encompassed measurements of circulating PLA2R antibody titer, circulating THSD7A antibody titer, hemoglobin (Hb), glucose (GLU), albumin (ALB), erythrocyte sedimentation rate (ESR), C-reactive protein (CRP), serum creatinine (sCr), uric acid (UA), and 24-hour urinary protein (24 h UTP). For patients in the malignant tumor group, additional data on the specific

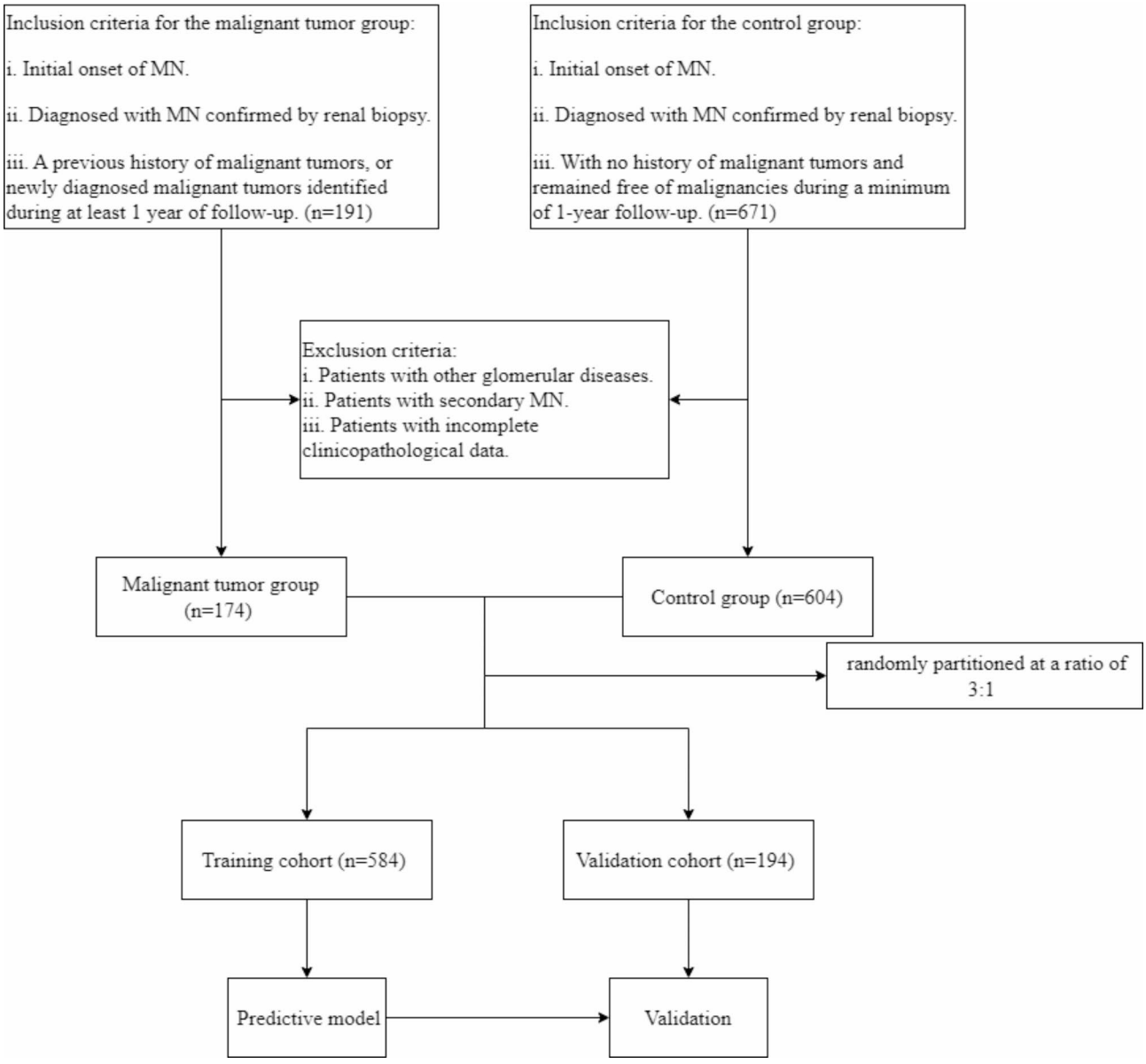

Fig. 1 Flow chart of the study

type of malignant tumor and the time interval between the diagnosis of MN and the occurrence of the malignant tumor were recorded.

Serum PLA2R antibody detection by ELISA KIT

Serum PLA2R antibody was collected in a medical database, and it was detected by ELISA Kit (Euroimmun, Germany) according to the instruction book. A serum PLA2R antibody level ≥ 14 U/ml was defined as a positive result.

Pathological data collection and definition

The renal tissue specimens were subject to light microscopy, immunofluorescence and electron microscopy. Results were first independently diagnosed by a primary nephropathologist and then evaluated by an advanced nephropathologist. In cases where inconsistencies arose, the final decision was entrusted to the senior nephropathologist. Ehrenreich-Churg's classification criteria were utilized to categorize IMN into pathological stages I to IV. To facilitate statistical analysis, when the stage fell between two criteria, the higher stage was assigned. For instance, stages I to II were classified as stage II. In addition, renal tubule atrophy, renal interstitial fibrosis, and renal arteriole injury were assessed using a semi-quantitative grading system. The extent of renal tubule atrophy and renal interstitial fibrosis was scored as follows: 0 points for no lesion, 1 point for < 25% lesion area,

2 points for 25–50% lesion area, and 3 points for >50% lesion area. Renal arteriole injury was scored as 0 points for no lesion, 1 point for thickening of the vascular wall, and 2 points for thickening of the vascular wall combined with any other vascular injury. Immunofluorescence staining intensity was considered negative for staining intensity < 1 + and positive for staining intensity ≥ 1+.

TRIPOD + AI guidelines

This study adheres to the TRIPOD (Transparent Reporting of a multivariable prediction model for Individual Prognosis or Diagnosis) + AI (Artificial intelligence) guidelines for reporting clinical prediction models [16]. We followed these guidelines to ensure that our methodology, model development, and performance evaluation are clearly and comprehensively reported (Supplementary Materials 1 and 2).

Statistical analysis

All statistical analyses were performed using SPSS software (version 21.0) and R statistical software (version 4.2.1; http://www.R-project.org). A p-value of less than 0.05 was considered statistically significant. Pairwise deletion was used to exclude only the variable pairs with missing values, retaining all other available data for analysis. Quantitative variables with normal distributions were expressed as mean ± standard deviation (SD). Depending on the homogeneity of variance, comparisons between two groups were conducted using either a t-test or a corrected t-test. Quantitative variables with non-normal distributions were reported as median and interquartile range [M (P25, P75)], and the Wilcoxon rank-sum test was used for comparisons. Categorical variables were presented as frequency and percentage [n (%)], and comparisons between groups were performed using the chi-square test. The data were randomly divided into training and validation cohorts in a 3:1 ratio using the R programming language. The training cohort was used to develop the predictive model, while the validation cohort served for internal validation. Univariate logistic regression analysis was conducted to identify potential risk factors for malignant tumors. Variance inflation factor (VIF) analysis was employed to detect multicollinearity among variables, with VIF ≥ 10 indicating high multicollinearity. Identified variables were then included in a multivariate logistic regression analysis to determine independent risk factors. The nomogram and predictive equation were constructed using the "rms" R package. Model performance was evaluated in both the training and validation cohorts. Discrimination ability was assessed using receiver operating characteristic (ROC) curves and the area under the ROC curve (AUC). An AUC > 0.90 indicated excellent performance; 0.80–0.89, good; 0.70–0.79, fair; and < 0.70, poor. Calibration of the model was assessed using calibration curves based on 500 bootstrap samples and the Brier score. Clinical utility was determined using decision curve analysis (DCA), which quantified the net benefit of the model at different threshold probabilities for both training and validation cohorts.

Results

The distribution of malignant tumors and the time interval from diagnosis of MN

A total of 174 patients (89 men and 85 women) with a median age of 58 (47,67) years at the time of MN diagnosis were enrolled in the malignant tumor group. As shown in Fig. 2, 64.9% of patients were diagnosed with malignant tumors within one year before or after the diagnosis of MN. Additionally, 31.6% of patients were diagnosed with malignant tumors at the time of MN diagnosis, 32.2% were diagnosed after MN diagnosis, and 36.2% were diagnosed before MN diagnosis. The prevalence of malignant tumors is detailed in Table 1. It was observed to be highest in thyroid cancer (41 cases, 23.6%) and lung cancer (34 cases, 19.5%), followed by prostate cancer (10 cases, 5.8%), gastric cancer (10 cases, 5.8%), and colorectal cancer (10 cases, 5.8%). Non-solid tumors were also identified, including multiple myeloma (9 cases, 5.2%), leukemia (6 cases, 3.5%)), lymphoma (4 cases, 2.3%), and myelodysplastic syndrome (1 case, 0.6%).

Comparison of the baseline characteristics between MN patients complicated with and without malignant tumors

The demographic and clinicopathological characteristics of MN patients complicated with and without malignant tumors are summarized in Table 2. The median ages of the two groups were 58 (47–66) years and 48 (37–58) years, respectively, indicating that MN patients with malignant tumors were significantly older than those without malignant tumors. No statistically significant difference in gender distribution was observed between the two groups. In terms of laboratory findings, MN patients with malignant tumors exhibited lower circulating anti-PLA2R antibody titers, lower positive rates of circulating anti-PLA2R antibodies, and reduced Hb levels. Additionally, these patients had higher levels of GLU, ESR, CRP, and 24hUTP. However, no significant differences were noted in circulating anti-THSD7A antibody titers, ALB, sCr, or UA levels between the groups. Regarding renal pathological parameters, MN patients with malignant tumors exhibited more advanced MN staging, more severe tubular atrophy, interstitial fibrosis, and arteriolar injury. Furthermore, these patients demonstrated higher positive rates for glomerular deposition of IgG, IgM, IgA, C3, C4, C1q, as well as IgG1, IgG2, IgG3, and PLA2R staining. Conversely, the deposition rate of IgG4 was significantly lower in the malignant tumor group.

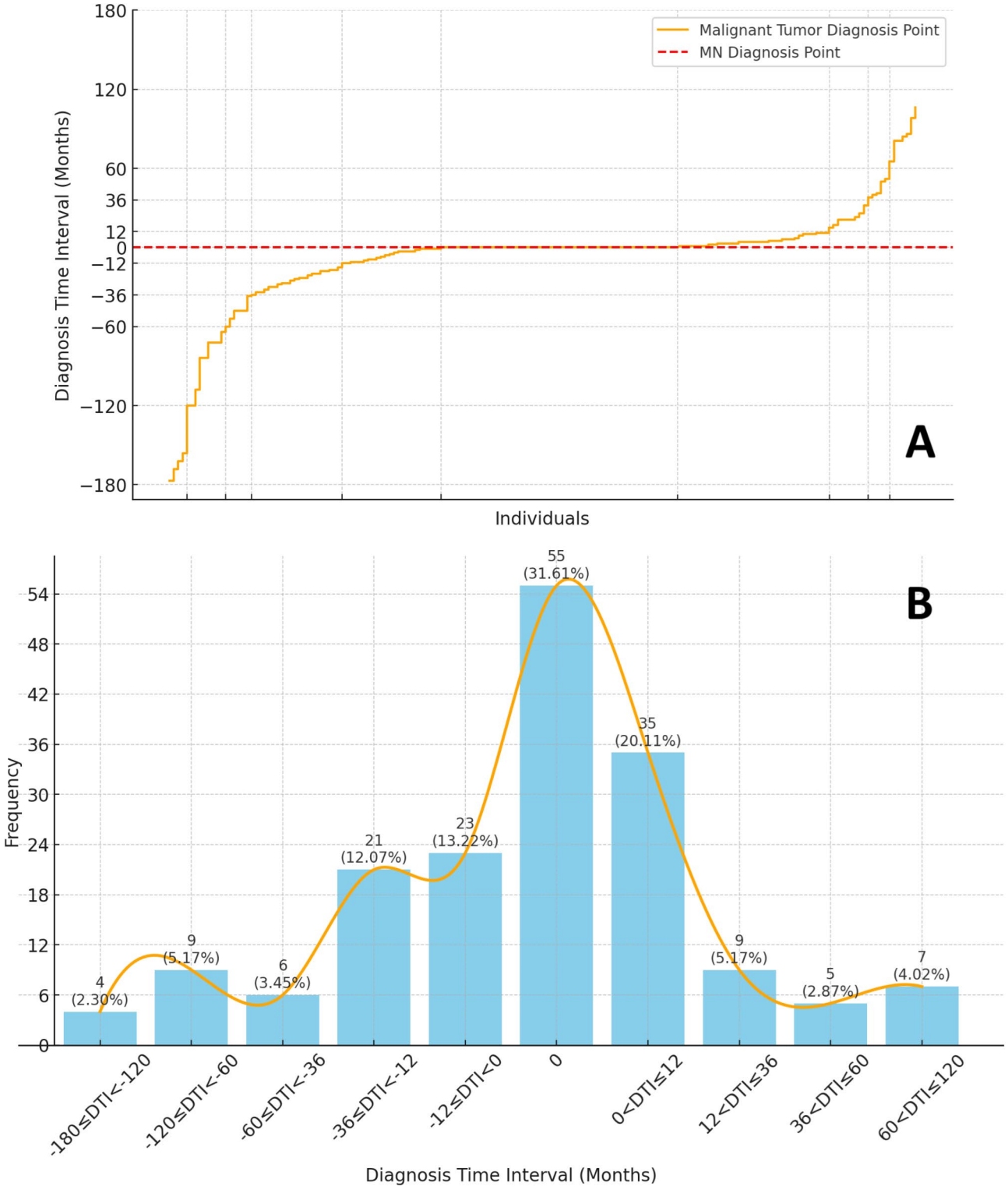

Fig. 2 Diagnosis time interval distribution for malignant tumors in patients with MN. (**A**) The cumulative plot of the diagnosis time interval for each individual, with the malignant tumor diagnosis point (orange) and MN diagnosis point (red dashed line) indicated. The X-axis represents individuals, with each width corresponding to their frequency, and the Y-axis represents the diagnosis time interval in months. (**B**) The histogram illustrating the frequency distribution of the diagnosis time intervals. The X-axis represents the grouped diagnosis time intervals (in months), and the Y-axis represents the frequency of individuals within each group

Table 1 Characteristics of patients in malignant tumor group

Malignant tumor type	Count	Male	Age at biospy
Thyroid cancer	41 (23.56)	13 (31.7)	50 (39, 59)
Lung cancer	34 (19.54)	24 (70.6)	58 ± 13
Prostate cancer	10 (5.75)	10 (100)	66 (60, 70)
Gastric cancer	10 (5.75)	5 (50)	61 (54, 67)
Colorectal cancer	10 (5.75)	7 (70)	56 (50, 63)
Multiple myeloma	9 (5.17)	7 (77.8)	63 (49, 69)
Breast cancer	7 (4.02)	0 (0)	62 (49, 67)
Uterine cancer	7 (4.02)	0 (0)	58 (56, 60)
Leukaemia	6 (3.45)	2 (33.3)	45 (34, 69)
Bladder cancer	5 (2.87)	2 (40)	64 (54, 72)
Esophageal cancer	5 (2.87)	4 (80)	58 (45, 61)
Cervical cancer	4 (2.30)	4 (100)	51 (46, 60)
Lymphoma	4 (2.30)	2 (50)	63 (49, 69)
Renal cancer	4 (2.30)	3 (75)	60 (50, 64)
Liver cancer	3 (1.72)	3 (100)	66 (59, 67)
Ovarian cancer	1 (0.57)	0 (0)	67
Brain cancer	2 (1.15)	1 (50)	53, 58
Cholangiocarcinoma	1 (0.57)	1 (100)	70
Pancreatic cancer	1 (0.57)	0 (0)	33
Testicular seminoma	1 (0.57)	1 (100)	46
Malignant teratoma	1 (0.57)	0 (0)	52
Adrenal Cancer	1 (0.57)	1 (100)	62
Myelodysplastic syndrome	1 (0.57)	1 (100)	38
Small intestinal cancer	1 (0.57)	0 (0)	68
Other	5 (2.87)	2 (40)	46 (39, 67)

Screening for predictive factors associated with malignant tumors in MN patients

A total of 778 patients were randomly allocated into a training cohort ($n = 584$) and a validation cohort ($n = 194$) at a 3:1 ratio. The demographic and clinicopathological baseline characteristics of the two cohorts are summarized in the Supplementary Table. No significant differences were observed between two cohorts across all studied indicators ($P > 0.05$). Multivariate logistic regression analysis was conducted, incorporating all parameters with a P-value < 0.05 from the univariate analyses. Variance inflation factor (VIF) values for the independent variables ranged from 1.178 to 1.660, indicating the absence of significant multicollinearity issues. The final analysis identified the following factors as independent predictors of malignant tumors in MN patients: increased deposition of glomerular IgA (OR 2.980; 95% CI 1.071–8.291; $P = 0.036$), IgG1 (OR 2.535; 95% CI 1.367–4.703; $P = 0.003$), IgG2 (OR 5.185; 95% CI 1.689–15.917; $P = 0.004$), IgG3 (OR 3.558; 95% CI 1.417–8.934; $P = 0.007$), and PLA2R (OR 3.167; 95% CI 1.559–6.431; $P = 0.001$). Conversely, deposition of glomerular IgG4 (OR 0.435; 95% CI 0.194–0.974; $P = 0.043$) was found to be inversely associated with the risk of malignant tumors (Table 3).

Construction and validation of the nomogram

Based on the results of the multivariate logistic regression analysis, six independent predictors—glomerular deposition of IgA, IgG1, IgG2, IgG3, IgG4, and PLA2R—were incorporated into the construction of a nomogram to estimate the likelihood of malignant tumors in MN patients at the time of initial diagnosis (Fig. 3). The diagnostic performance of the nomogram was evaluated using ROC curves, calibration curves, and DCA curves for both the training and validation cohorts. The nomogram demonstrated excellent discriminatory ability, achieving an AUC of 0.893 (95% CI: 0.854–0.930) in the training cohort and 0.943 (95% CI: 0.895–0.990) in the validation cohort (Fig. 4A/4B). Calibration curves showed a high degree of consistency between the predicted probabilities generated by the nomogram and the observed probabilities, with results closely aligning with the ideal diagonal line (Fig. 5A/5B). Additionally, DCA curves highlighted the nomogram's ability to deliver a positive net benefit across a range of threshold probabilities (0 to 1), underscoring its significant potential for clinical application (Fig. 6A/6B).

Sensitivity analysis

To further assess the robustness of the predictive model, we conducted a sensitivity analysis to evaluate whether the model's performance would differ if medical records outside the ± 12-month window were unavailable. One group used the complete set of all patients, while the other group used only data within the ± 12-month window. The ROC values for these two groups were 0.898 (95% CI: 0.864–0.932) and 0.903 (95% CI: 0.866–0.941), respectively. These results indicate that the model's diagnostic accuracy remains robust across different time frames.

Discussion

To the best of our knowledge, this study represents the largest single-center investigation to date focused on predicting the risk of malignant tumors in patients with MN. Unlike previous studies on malignancy-associated MN, which often restricted the timeframe for the occurrence of malignant tumors, our study took a broader approach by examining the overarching association between MN and malignancy. Importantly, we made a pioneering attempt to develop a predictive model that integrates renal pathological indicators. This model demonstrates high diagnostic performance, offering a robust tool for predicting the occurrence of malignant tumors in patients diagnosed with MN.

Our study revealed that among MN patients with malignant tumors, approximately 64.9% were diagnosed with malignancies concurrently with MN (within 12 months before or after the MN diagnosis). In total, 174

Table 2 Baseline characteristics of MN patients with or without malignant tumors

	Malignant tumor group (*n* = 174)	Control group (*n* = 604)	*P* value
Male (%)	89 (51.1)	346 (57.4)	0.145
Age (years)	58 (47, 66)	48 (37, 58)	< 0.001
PLA2R Ab (U/mL)	15.10 (2.10, 83.65)	29.5 (9.33, 84.58)	0.001
PLA2R Ab (+)	76 (51.0)	338 (66.1)	0.001
THSD7A Ab (ng/mL)	58.10 (24.40, 162.90)	59.80 (38.30, 97.20)	0.885
Hb (g/L)	123.00 (108.00, 136.00)	131.00 (121.00, 142.85)	< 0.001
GLU (mmol/L)	4.85 (4.41, 5.33)	4.47 (4.10, 4.99)	< 0.001
ALB (g/L)	27.00 (22.20, 31.88)	26.10 (22.20, 31.20)	0.258
ESR (mm/h)	49.00 (19.25, 75.00)	26.00 (14.00, 43.00)	< 0.001
CRP (mg/L)	1.39 (0.50, 3.38)	0.90 (0.10, 1.90)	< 0.001
sCr (umol/L)	65.50 (53.00, 87.00)	65.00 (55.00, 76.00)	0.064
UA (umol/L)	304.00 (252.00, 372.75)	310.00(258.00, 373.00)	0.634
24hUTP (g)	4.90 (2.64, 8.10)	3.86 (2.10, 6.23)	0.003
Pathological stage:			< 0.001
1	11 (7.4)	95 (15.7)	
2	95 (63.8)	398 (65.9)	
3	39 (26.2)	111 (18.4)	
4	4 (2.7)	0 (0)	
Tubular atrophy:			< 0.001
0	61 (37.7)	348 (57.6)	
1	39 (24.1)	61 (10.1)	
2	35 (21.6)	100 (16.6)	
3	27 (16.7)	95 (15.7)	
Interstitial fibrosis:			0.008
0	80 (49.4)	333 (55.1)	
1	42 (25.9)	101 (16.7)	
2	33 (20.4)	159 (26.3)	
3	7 (4.3)	11 (1.8)	
Renal arteriole injury:			< 0.001
0	26 (16.0)	270 (44.7)	
1	31 (19.1)	162 (26.8)	
2	105 (64.8)	172 (28.5)	
IgG			< 0.001
0	5 (3.1)	14 (2.3)	
1	4 (2.5)	58 (9.6)	
2	73 (45.1)	391 (64.7)	
3	75 (46.3)	141 (23.3)	
4	5 (3.1)	0 (0)	
IgM			< 0.001
0	43 (28.7)	389 (64.4)	
1	52 (34.7)	151 (25.0)	
2	54 (36.0)	64 (10.6)	
3	1 (0.7)	0 (0)	
IgA			< 0.001
0	119 (73.5)	591 (97.8)	
1	26 (16.0)	7 (1.2)	
2	17 (10.5)	6 (1.0)	
C3			< 0.001
0	49 (30.2)	267 (44.2)	
1	32 (19.8)	183 (30.3)	
2	73 (45.1)	149 (24.7)	
3	8 (4.9)	5 (0.8)	
C4			< 0.001

Table 2 (continued)

	Malignant tumor group (*n* = 174)	Control group (*n* = 604)	*P* value
0	87 (59.2)	518 (85.8)	
1	40 (27.2)	69 (11.4)	
2	20 (13.6)	17 (2.8)	
C1q			< 0.001
0	120 (74.5)	579 (95.9)	
1	28 (17.4)	23 (3.8)	
2	13 (8.1)	2 (0.3)	
IgG1			< 0.001
0	42 (29.0)	345 (57.1)	
1	46 (31.7)	152 (25.2)	
2	51 (35.2)	104 (17.2)	
3	6 (4.1)	3 (0.5)	
IgG2			< 0.001
0	84 (58.3)	575 (95.2)	
1	40 (27.8)	26 (4.3)	
2	20 (13.9)	3 (0.5)	
IgG3			< 0.001
0	105 (72.4)	547 (90.6)	
1	21 (14.5)	35 (5.8)	
2	19 (13.1)	22 (3.6)	
IgG4			< 0.001
0	30 (20.5)	0 (0)	
1	11 (7.5)	73 (12.1)	
2	71 (48.6)	395 (65.4)	
3	34 (23.3)	136 (22.5)	
PLA2R			< 0.001
0	35 (28.2)	215 (50.4)	
1	15 (12.1)	114 (26.7)	
2	74 (59.7)	98 (23.0)	

MN patients with malignant tumors were included in this study. Thyroid cancer (42 cases, 21.6%) and lung cancer (37 cases, 19.1%) were the most frequently observed malignancies, followed by colorectal cancer (12 cases, 6.2%), prostate cancer (11 cases, 5.7%), and gastric cancer (10 cases, 5.2%). These findings are generally consistent with those reported in previous studies [17], although new evidence highlights thyroid cancer as the most prevalent malignancy among MN patients. Furthermore, non-solid tumors, including multiple myeloma (9 cases, 4.6%) and leukemia (6 cases, 3.0%), were also identified, underscoring the diverse spectrum of malignancies associated with MN.

We observed that the average age of MN patients with malignant tumors was significantly higher compared to those without malignant tumors, consistent with findings from previous studies [12, 13, 14, 15]. Additionally, MN patients with malignant tumors demonstrated lower levels of Hb, higher levels of GLU, ESR, CRP, and 24hUTP, alongside more advanced renal pathological stages and more severe glomerular injury. These findings may be attributable to systemic inflammation induced by malignant tumors and the progressive deterioration of renal function.

PLA2R and THSD7A have been identified as the principal pathogenic podocyte antigens in IMN. Subsequent studies revealed that glomerular PLA2R and THSD7A antigens, as well as circulating anti-PLA2R and THSD7A antibodies, are also present in patients with malignancy-associated MN [10, 13, 14]. However, conflicting evidence exists regarding the ability of PLA2R and THSD7A to differentiate between malignancy-associated MN and IMN. Our findings indicate that MN patients with negative circulating PLA2R antibodies but positive glomerular PLA2R deposition are more likely to develop malignant tumors. This contrasts with a study by Zhang et al., which analyzed a cohort of 12 malignancy-associated MN patients and 257 IMN patients, concluding that negative circulating anti-PLA2R antibodies and absence of glomerular PLA2R deposition may suggest an association with malignant tumors [14]. In our study, 124 out of 174 MN patients with malignant tumors and 427 out of 604 patients in the control group underwent glomerular PLA2R testing, with positivity rates of 72% and 50%, respectively. While PLA2R-positive cases are typically

Table 3 Identification of potential risk factors of MN complicated with malignant tumors by univariate and multivariate regression analysis

	Univariable			Multivariable		
	OR	**95%CI**	***P* value**	**OR**	**95%CI**	***P* value**
Male (%)	1.232	0.933–1.820	0.296			
Age (years)	1.041	1.026–1.057	< 0.001	1.026	0.987–1.066	0.201
PLA2R Ab (RU/mL)	0.999	0.999-1.000	0.300			
PLA2R Ab (+)	0.555	0.361–0.853	0.007	0.612	0.200-1.874	0.390
THSD7A Ab (ng/mL)	1.003	0.999–1.006	0.174			
Hb (g/L)	0.977	0.966–0.987	< 0.001	0.974	0.946–1.003	0.077
GLU (mmol/L)	1.367	1.090–1.715	0.007	1.268	0.812–1.979	0.296
ALB (g/L)	1.020	0.991–1.051	0.183			
ESR (mm/h)	1.018	1.0111.024	< 0.001	1.009	0.990–1.028	0.360
CRP (mg/L)	1.030	1.011–1.050	0.002	1.016	0.982–1.051	0.371
sCr (umol/L)	1.019	1.009–1.028	< 0.001	1.003	0.990–1.016	0.675
UA (umol/L)	1.001	0.998–1.003	0.530			
24hUTP (g)	1.059	1.004–1.117	0.034	1.032	0.883–1.206	0.692
Pathological stage	1.763	1.247–2.493	0.001	1.555	0.683–3.539	0.293
Tubular atrophy	1.194	1.009–1.414	0.040	0.798	0.510–1.248	0.323
Interstitial fibrosis	1.107	0.888–1.380	0.365			
Renal arteriole injury	2.592	1.978–3.398	< 0.001	1.560	0.797–3.052	0.194
IgG	2.551	1.791–3.632	< 0.001	2.147	0.957–4.815	0.064
IgM	2.941	2.240–3.863	< 0.001	1.053	0.524–2.118	0.884
IgA	7.148	3.923–13.023	< 0.001	2.980	1.071–8.291	0.036
C3	1.756	1.385–2.227	< 0.001	0.819	0.422–1.590	0.556
C4	2.872	2.031–4.062	< 0.001	0.737	0.289–1.878	0.523
C1q	7.018	3.877–12.706	< 0.001	1.162	0.205–6.567	0.865
IgG1	1.935	1.511–2.480	< 0.001	2.535	1.367–4.703	0.003
IgG2	8.476	4.929–14.574	< 0.001	5.185	1.689–15.917	0.004
IgG3	2.353	1.694–3.270	< 0.001	3.558	1.417–8.934	0.007
IgG4	0.506	0.379–0.674	< 0.001	0.435	0.194–0.974	0.043
PLA2R	2.217	1.670–2.944	< 0.001	3.167	1.559–6.431	0.001

found in approximately 70% of primary MN patients, the relatively lower PLA2R positivity rate in the control group raises concerns. This inconsistency may be influenced by factors such as testing methodology, sample selection, the single-center nature of our study, or the heterogeneity of the disease itself. These differences may affect the interpretation of our results, and we recommend that future studies further investigate this aspect to better understand the potential impact of glomerular PLA2R deposition on malignancy. Additionally, recent studies investigating the incidence of malignant tumors in THSD7A-associated MN patients have reported similarly conflicting results [14, 18]. Notably, our study did not assess glomerular THSD7A deposition, and no significant difference in circulating anti-THSD7A antibodies was observed between the two cohorts. Thus, the relationship between THSD7A-associated MN and malignancy remains an open question requiring further investigation.

The granular deposition of IgG along capillary walls is a hallmark of renal immunofluorescence in MN. Human IgG is divided into four subclasses (IgG1, IgG2, IgG3, and IgG4) based on variations in their heavy chain antigens. Distinct pathogenic antigens can lead to specific glomerular IgG subclass deposition patterns, which aid in identifying the type and etiology of glomerular nephropathy [11]. For instance, the antibodies targeting PLA2R and THSD7A are predominantly of the IgG4 subclass, which corresponds to characteristic IgG4-dominant glomerular deposition in IMN. Nevertheless, the role of different IgG subclasses in MN pathogenesis remains unclear, and prior studies on glomerular IgG subclass distribution have yielded inconsistent results. Ohtani et al. compared glomerular IgG subclass deposition in 10 malignancy-associated MN and 15 IMN patients, reporting significantly higher glomerular immunofluorescence intensity of IgG1 and IgG2 in the malignancy group, while IgG4 deposition was similar to that in IMN [11]. Conversely, Qu et al. suggested that the absence of glomerular IgG4 deposition could serve as an independent predictor for malignancy, based on their study of 8 malignancy-associated MN and 42 IMN patients [12]. Lönnbro-Widgren et al. later demonstrated a significant correlation between glomerular IgG4 and PLA2R deposition in malignancy-associated

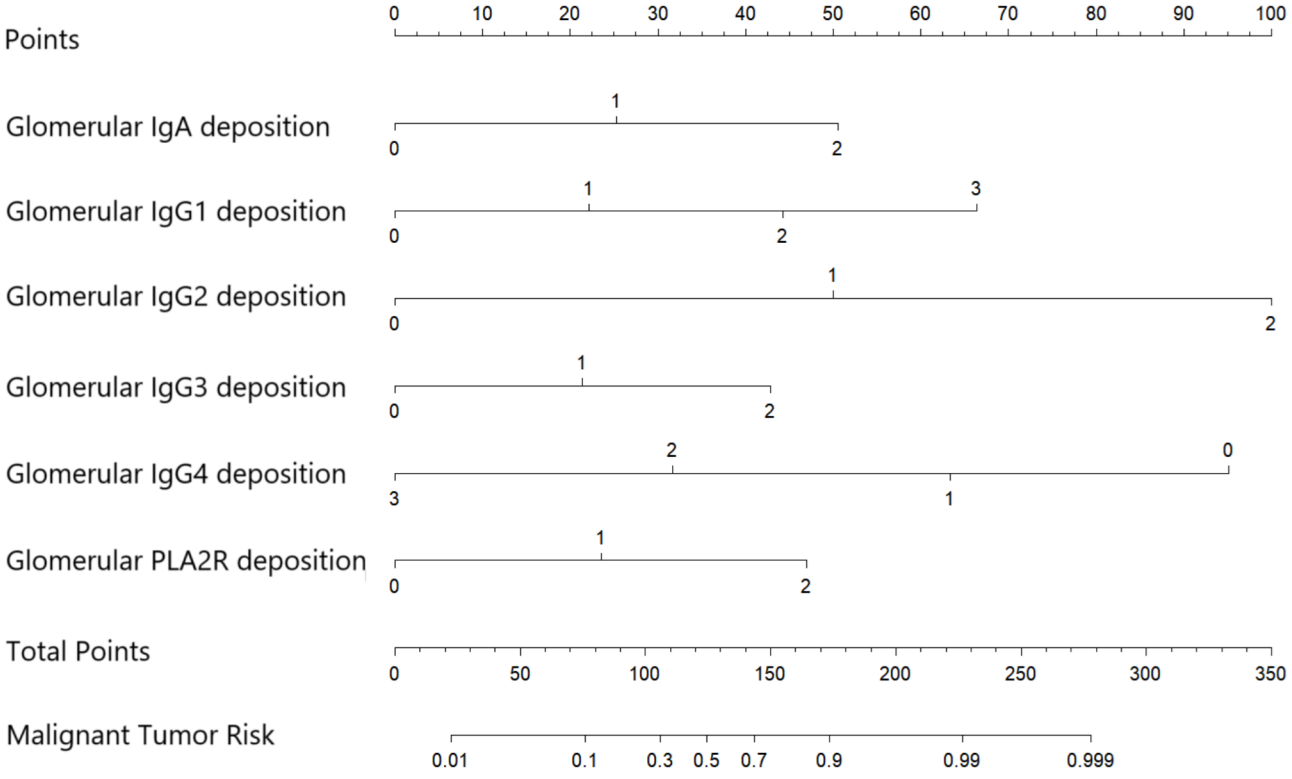

Fig. 3 Nomogram predicting the risk of malignant tumors in MN patients. The nomogram incorporates glomerular IgA, IgG1, IgG2, IgG3, IgG4, and PLA2R deposition as predictors. For each predictor, the corresponding point value is determined along the top scale, and the total points are calculated by summing the points for each predictor. The total points are then mapped to the predicted malignant tumor risk on the bottom scale

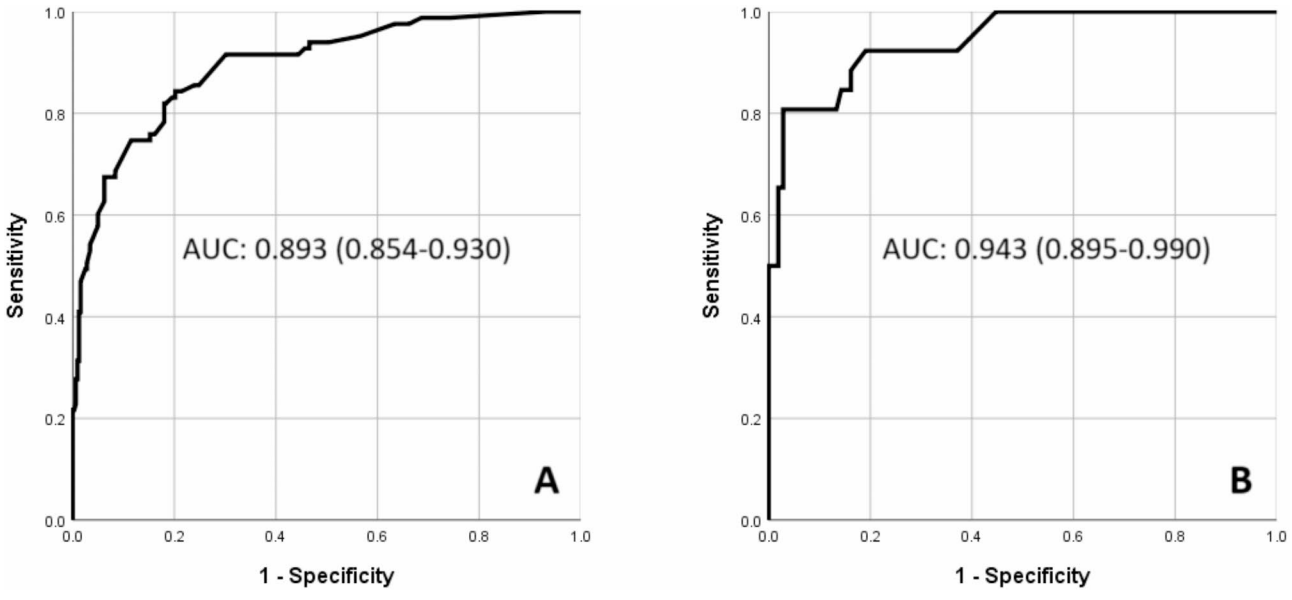

Fig. 4 ROC curves for the predictive model. (**A**) Training cohort. (**B**) Validation cohort

MN but found no significant differences in other IgG subclasses between 16 malignancy-associated MN and 69 IMN patients [13]. In the present study, leveraging the largest sample size to date, we observed that increased glomerular deposition of IgG1, IgG2, and IgG3, along with decreased IgG4 deposition, were strongly associated with malignancy-associated MN. Furthermore, these patterns were identified as independent risk factors for predicting the occurrence of malignant tumors. These findings provide robust evidence to resolve some of the

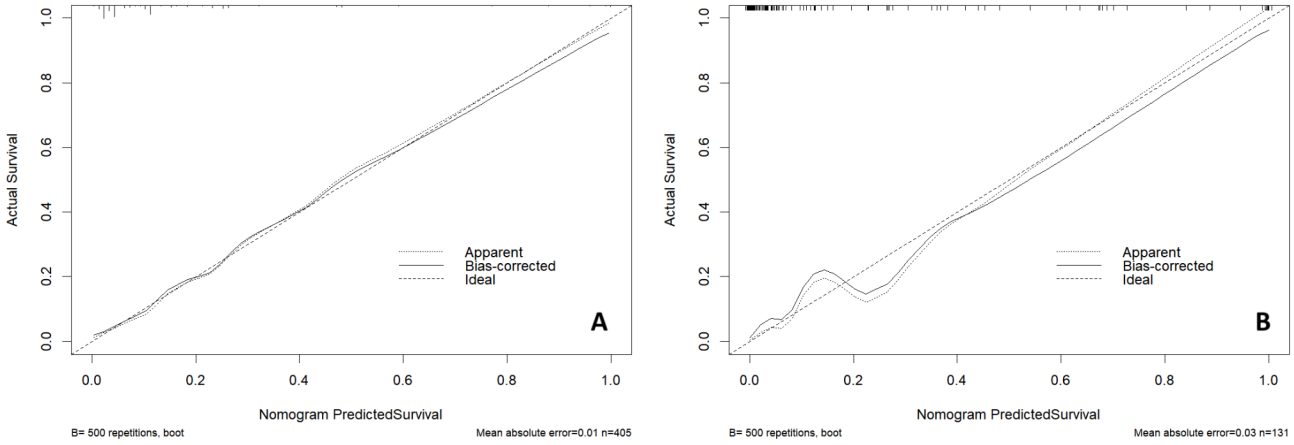

Fig. 5 Calibration curves for the predictive model. (**A**) Training cohort. (**B**) Validation cohort. The X-axis represents the predicted probability, and the Y-axis represents the actual occurrence probability. The diagonal dashed line labeled "Ideal" represents the ideal scenario where the predicted probabilities match the actual probabilities. The dashed line labeled "Apparent" represents the consistency between the predicted probabilities (calculated once based on the model) and the actual probabilities, while the solid line labeled "Bias-corrected" represents the result after bootstrapping the data used to construct the model

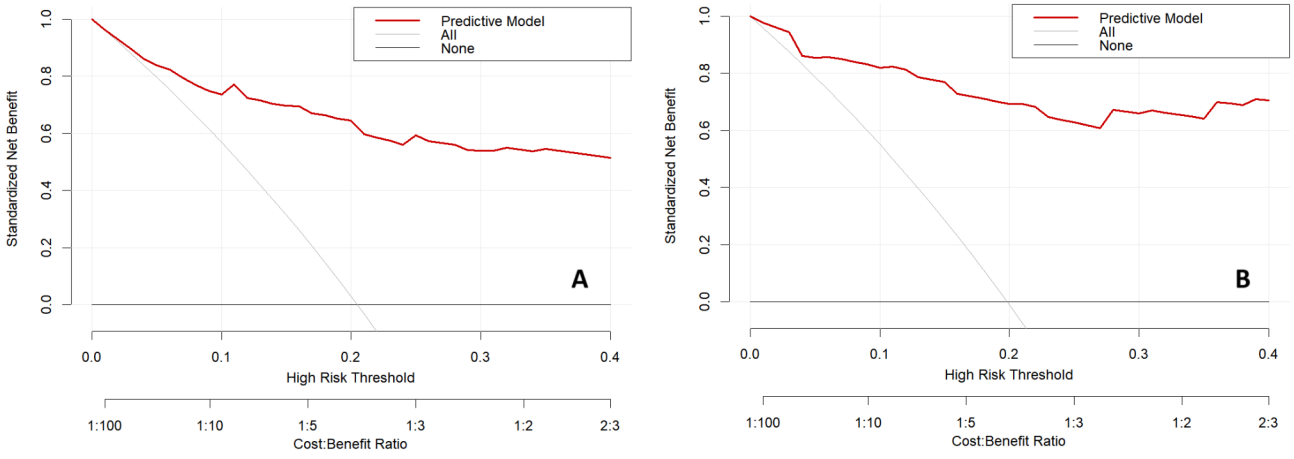

Fig. 6 DCA curves for the predictive model. (**A**) Training cohort. (**B**) Validation cohort. The X-axis represents the high-risk threshold, which is the risk required to drive a specific treatment (ranging from 0 to 1). The Y-axis represents the standardized net benefit, which shows the net benefit across a range of threshold probabilities. The red line represents the predictive model, the gray line represents the "All" strategy (treating all patients), and the black line represents the "None" strategy (treating no patients)

controversies regarding the role of IgG subclasses in MN and underline their potential diagnostic value. However, we observed a puzzling result where, after adjusting for all IgG subclasses and PLA2R deposition in the multivariate logistic regression, PLA2R remained an independent predictor of malignant tumors in MN, while IgG4 was inversely correlated with this risk. This finding seems counterintuitive, as PLA2R-positive MN is primarily IgG4-restricted and is generally not associated with malignancy. This discrepancy may reflect the heterogeneous immune response, where malignancy could influence the immune system in a way that alters the typical distribution of IgG subclasses, leading to lower IgG4 levels. Tumor-associated immune mechanisms may contribute to shifts in the production of specific IgG subclasses, resulting in the observed difference.

Different IgG subclasses demonstrate varying capacities to fix complement, and the complement activation pathways differ among various disease types [19, 20, 21]. However, our understanding of the precise role of complement activation in the pathogenesis of MN remains limited. C1q, the initial component of the classical complement pathway, serves as a key marker for the activation of this pathway [22]. Its elevated expression indicates complement activation through classical pathways. Moreover, in comparison to IMN patients, those with malignancy-associated MN exhibited significantly greater deposition of C3 and C4. This finding suggests enhanced formation of membrane attack complexes,

leading to more severe renal damage. These observations align with our findings of heightened systemic inflammation and increased 24hUTP in the malignant tumor group.

We also observed that glomerular IgA deposition is an independent risk factor in MN patients complicated with malignant tumors. This finding is consistent with previous studies that reported a higher incidence of glomerular IgA deposition in cancer patients. For example, one study documented glomerular IgA deposition in 8 out of 11 autopsied patients with malignancies such as lung, stomach, colon, and pancreatic cancer [23]. Similarly, another study identified glomerular IgA deposition in 3 out of 18 lung cancer patients [24]. Furthermore, other studies have reported that the co-deposition of IgA and IgG in some MN patients is associated with secondary factors such as autoimmune diseases, hepatitis B infection, or kidney transplantation [25]. These associations suggest that malignancies may influence the renal immune microenvironment, although the precise mechanisms remain unclear.

Wang et al. previously developed the first predictive model for malignancy-associated MN, incorporating 62 MN cases and 385 IMN cases [26]. However, their findings did not demonstrate statistically significant differences in key pathological indicators, such as PLA2R and IgG subtype deposition, as well as tubular atrophy and interstitial fibrosis. The discrepancies in findings and patient characteristics between the two studies may be attributed to differences in recruitment periods and inclusion criteria. In the present retrospective study, we developed and validated a risk predictive model for malignant tumors in MN patients based on critical pathological indicators, including the deposition of glomerular IgA, IgG1, IgG2, IgG3, IgG4, and PLA2R. The model exhibited excellent diagnostic performance, with AUC of 0.893 in the training cohort and 0.943 in the validation cohort. Furthermore, the model demonstrated robust calibration capability and substantial clinical utility upon validation.

Our study has several limitations. First, as a retrospective study, it relies on medical records as the primary data source. This inherently limits the availability of comprehensive clinical and pathological information for all patients. For example, some MN patients complicated with malignant tumors did not undergo renal biopsy and were therefore not included in the analysis. Additionally, certain previously identified risk factors were not available, such as cystatin C levels, the extent of glomerular leukocyte infiltration, and glomerular expression of NELL1 and THSD7A. Second, the follow-up period was relatively short. For the non-cancer group, although malignancy was not identified after one year of follow-up, it is important to note that this does not completely exclude the possibility of "subclinical" malignancy or other potential triggers for MN. Third, this is a single-center study without external validation. Consequently, the generalizability of the predictive model to other populations remains uncertain. Future studies involving multi-center, multi-region, and larger sample sizes are essential to verify the applicability and robustness of our findings. Fourth, existing studies, including ours, have primarily focused on comparing the clinicopathological characteristics between idiopathic IMN and MN complicated with malignant tumors or malignancy-associated MN. Further progress could benefit from integrating additional investigative methods. For example, a multi-omics approach incorporating DNA, RNA, and protein profiling from serum samples of these patients could provide deeper insights into the molecular mechanisms underlying these associations.

Conclusions

Based on the largest cohort to date, our study revealed that MN patients with malignant tumors are characterized by older age and more severe clinicopathological manifestations. Notably, lower circulating anti-PLA2R antibody levels, increased glomerular PLA2R deposition, heightened glomerular IgG1, IgG2, and IgG3 deposition, and reduced glomerular IgG4 deposition were identified as potential indicators for the occurrence of malignant tumors in MN patients. Additionally, we developed a robust predictive model for malignant tumors in MN patients, validated to demonstrate high accuracy.

Supplementary Information

The online version contains supplementary material available at https://doi.org/10.1186/s12882-025-04053-y.

Supplementary Material 1

Supplementary Material 2

Acknowledgements

We wish to thank Department of Medical Records (Professor Feng Chen) and Department of Pathology of The First Affiliated Hospital of Zhengzhou University for supporting.

Author contributions

Y. Z. and S. S. are considered co-first authors and have equally contributed to the conception, execution, and finalization of this work. W. Z. and H. T. contributed to data organization and verification. Z. Z. designed the study and revised the manuscript. All authors read and approved the final manuscript.

Funding

This study was supported by the General Project of Henan Natural Science Foundation (232300420034), the National Natural Science Foundation of China for the Youth (81600555), and the General Project of China Postdoctoral Science Foundation (2018M640684).

Data availability

No datasets were generated or analysed during the current study.

Data sharing statement
Raw data used during the current study are available from the corresponding author on reasonable request for noncommercial use.

Declarations

Ethics approval and consent to participate
Due to the retrospective and anonymized nature of the study, the ethics committee of the First Affiliated Hospital of Zhengzhou University exempted this study from ethical approval.

Consent for publication
Not applicable.

Competing interests
The authors declare no competing interests.

Conflict of interest
The authors declare no competing interests.

Received: 21 July 2024 / Accepted: 3 March 2025
Published online: 22 March 2025

References

1. Hu R, Quan S, Wang Y, et al. Spectrum of biopsy proven renal diseases in central China: a 10-year retrospective study based on 34,630 cases. Sci Rep. 2020;10(1):10994.
2. Hou JH, Zhu HX, Zhou ML, et al. Changes in the spectrum of kidney diseases: an analysis of 40,759 Biopsy-Proven cases from 2003 to 2014 in China. Kidney Dis (Basel). 2018;4(1):10–9.
3. Lee JC, Yamauchi H, Hopper J Jr. The association of cancer and the nephrotic syndrome. Ann Intern Med. 1966;64(1):41–51.
4. Lefaucheur C, Stengel B, Nochy D, et al. Membranous nephropathy and cancer: epidemiologic evidence and determinants of high-risk cancer association. Kidney Int. 2006;70(8):1510–7.
5. Beck LH Jr. Membranous nephropathy and malignancy. Semin Nephrol. 2010;30(6):635–44.
6. Burstein DM, Korbet SM, Schwartz MM. Membranous glomerulonephritis and malignancy. Am J Kidney Dis. 1993;22(1):5–10.
7. Murtas C, Ghiggeri GM. Membranous glomerulonephritis: histological and serological features to differentiate cancer-related and non-related forms. J Nephrol. 2016;29(4):469–78.
8. Beck LH Jr, Bonegio RG, Lambeau G, et al. M-type phospholipase A2 receptor as target antigen in idiopathic membranous nephropathy. N Engl J Med. 2009;361(1):11–21.
9. Tomas NM, Beck LH Jr, Meyer-Schwesinger C, et al. Thrombospondin type-1 domain-containing 7A in idiopathic membranous nephropathy. N Engl J Med. 2014;371(24):2277–87.
10. Zhang C, Zhang M, Chen D, et al. Features of phospholipase A2 receptor and thrombospondin type-1 domain-containing 7A in malignancy-associated membranous nephropathy. J Clin Pathol. 2019;72(10):705–11.
11. Ohtani H, Wakui H, Komatsuda A, et al. Distribution of glomerular IgG subclass deposits in malignancy-associated membranous nephropathy. Nephrol Dial Transpl. 2004;19(3):574–9.
12. Qu Z, Liu G, Li J, et al. Absence of glomerular IgG4 deposition in patients with membranous nephropathy May indicate malignancy. Nephrol Dial Transpl. 2012;27(5):1931–7.
13. Lönnbro-Widgren J, Ebefors K, Mölne J, et al. Glomerular IgG subclasses in idiopathic and malignancy-associated membranous nephropathy. Clin Kidney J. 2015;8(4):433–9.
14. Zhang D, Zhang C, Bian F, et al. Clinicopathological features in membranous nephropathy with cancer: A retrospective single-center study and literature review. Int J Biol Markers. 2019;34(4):406–13.
15. Dong H, Feng Z. Clinical and immunopathological analysis of patients with tumor-associated membranous nephropathy. China Med Herald. 2022;19(16):109–12. (in Chinese with English abstract).
16. Collins GS, Moons KGM, Dhiman P, et al. TRIPOD + AI statement: updated guidance for reporting clinical prediction models that use regression or machine learning methods. BMJ. 2024;385:e078378.
17. Leeaphorn N, Kue-A-Pai P, Thamcharoen N, et al. Prevalence of cancer in membranous nephropathy: a systematic review and meta-analysis of observational studies. Am J Nephrol. 2014;40(1):29–35.
18. Xian L, Dong D, Luo J, et al. Expression of THSD7A in neoplasm tissues and its relationship with proteinuria. BMC Nephrol. 2019;20(1):332. Published 2019 Aug 23.
19. Nimmerjahn F, Ravetch JV. Divergent Immunoglobulin g subclass activity through selective Fc receptor binding. Science. 2005;310(5753):1510–2.
20. Vidarsson G, Dekkers G, Rispens T. IgG subclasses and allotypes: from structure to effector functions. Front Immunol. 2014;5:520. Published 2014 Oct 20.
21. Bruhns P. Properties of mouse and human IgG receptors and their contribution to disease models. Blood. 2012;119(24):5640–9.
22. Segawa Y, Hisano S, Matsushita M, et al. IgG subclasses and complement pathway in segmental and global membranous nephropathy. Pediatr Nephrol. 2010;25(6):1091–9.
23. Sinniah R. Mucin secreting cancer with mesangial IgA deposits. Pathology. 1982;14(3):303–8.
24. Endo Y, Hara M. Glomerular IgA deposition in pulmonary diseases. Kidney Int. 1986;29(2):557–62.
25. Yi G, Xie Q, Chen R, et al. Characteristics of membranous nephropathy patients with IgG and IgA Co-Deposits on capillary wall. J Am Soc Nephrol. 2021;32:466–466.
26. Wang T, Yu W, Wu F, et al. Construction of a nomogram discriminating Malignancy-Associated membranous nephropathy from idiopathic membranous nephropathy: A retrospective study. Front Oncol. 2022;12:914092.

Publisher's note